Deposited nanorod films for photonic crystal biosensor applications

Wei Zhang, Seok-min Kim, Nikhil Ganesh, Ian D. Block, Patrick C. Mathias, Hsin-Yu Wu, and Brian T. Cunningham[a)]
Nano Sensors Group, Micro and Nanotechnology Laboratory, University of Illinois at Urbana-Champaign, 208 North Wright Street, Urbana, Illinois 61801

(Received 15 October 2009; accepted 22 March 2010; published 29 June 2010)

Planar photonic crystals have been used as the basis of many biological sensing devices. Here, the authors successfully demonstrated that the combination of the photonic crystal structures and a dielectric nanorod coating prepared by the glancing-angle deposition technique can lead to significant increases in the device sensitivity. By incorporating a TiO_2 nanorod coating onto the label-free photonic crystal biosensor structure, the surface area of the device is increased. The results for detection of polymer films and proteins indicate up to a 5.5 fold enhancement of detected adsorbed mass density. © *2010 American Vacuum Society.* [DOI: 10.1116/1.3429595]

I. INTRODUCTION

In this work, the unique properties of planar photonic crystals (PCs) and dielectric nanorod films are combined to achieve enhanced sensitivities in label-free biosensors.

The planar PCs consist of a low-refractive-index (RI) polymer substrate with a subwavelength periodic modulation on its surface, overcoated with a high-RI dielectric coating. The structures are designed to work as a narrow-band reflectance filter whose resonant wavelength is dependent on the RI of the surrounding medium. Therefore, the resonant wavelength changes upon surface adsorption of molecules and the PCs can be used as label-free biosensors.

The nanorod films used in this study are fabricated by the glancing-angle deposition (GLAD) technique. Grown under conditions of glancing incidence of vapor flux and limited mobility of adatoms, these highly porous films are composed of isolated nanorods with a diameter of about 30 nm and an adjacent gap of about 15 nm. The feature sizes of the nanorods are small enough to prevent any significant scattering loss when used in optical devices, but are enough for a variety of proteins and molecules to penetrate into the structure and utilize the extra binding surface area. These features, along with the ease of fabrication, make these nanorod films ideal for optical biosensor applications.

A. Guided-mode resonance filters based on planar photonic crystals

Since their discovery by Wood[1,2] in 1902, guided-mode resonance filters (GMRFs) based on one-dimensional (1D) and two-dimensional PCs have attracted much attention.[3–14] Comprised of a subwavelength modulation in RI, such structures can produce complete exchange of energy between forward- and backward-propagating diffracted waves with smooth line shapes and arbitrarily low line widths.[5–7] PC structures displaying guided-mode resonances (GMRs) have been successfully used to develop optical filters,[15–18] polarizers,[6,19] light modulators,[20] wavelength-division multiplexing devices,[21] vertically emitting lasers,[22] light-emitting diodes with improved extraction efficiency,[23–25] optical nanoelectromechanical transducers,[26,27] humidity sensors,[28] label-free biosensors,[29–32] enhanced-fluorescence biosensors,[33–37] and substrates for surface-enhanced Raman spectroscopy.[38]

Figure 1(a) shows a representative example of a 1D planar PC designed to support GMRs. The structure is composed of a linear grating (50% duty cycle) in a low-RI polymer ($n_{substrate}=1.45$), with a period $\Lambda=400$ nm and a groove depth $h=100$ nm. The grating is coated with a high-RI TiO_2 ($n_{coating}=2.0$) of thickness $d_1=150$ nm. Using rigorous coupled-wave analysis,[39] the calculated reflection spectra of the 1D structure in Fig. 1(a) when illuminated with transverse electric (TE)-polarized (electric field along x-axis) and transverse magnetic (TM)-polarized (electric field along y-axis) white light at normal incidence (launch angle $\beta=0°$) are shown in Fig. 1(b).

The planar PC structures used in this study are fabricated with a cost-effective nanoreplica molding process.[40] Electron-beam lithography or photolithography were first used to define a negative image of the desired surface structure pattern, for example, a linear grating, onto a silicon (Si) master wafer [Fig. 2(a)]. Then a thin layer of liquid ultraviolet (UV)-curable polymer (UVCP) is squeezed between a flexible plastic substrate (typically polyethylene terephthalate) and the master wafer which acts as a molding tool [Fig. 2(b)]. After the epoxy is cured with UV illumination [Fig. 2(c)], the plastic sheet with the sensor structure is peeled away from the Si wafer [Fig. 2(d)]. A layer of titanium dioxide (TiO_2) with thickness d_1 is sputtered onto the sensor surface as the last step of sensor fabrication [Fig. 2(e)]. The biosensors are cut from the plastic sheet and attached with adhesive to form the bottom surface of standard microtiter plates,[41] microfluidic channels,[42,43] or the top surface of microscope glass slides.[37,44,45] Using this process, the desired device structure can be fabricated into very large areas efficiently and cost effectively.

[a)]Electronic mail: bcunning@illinois.edu

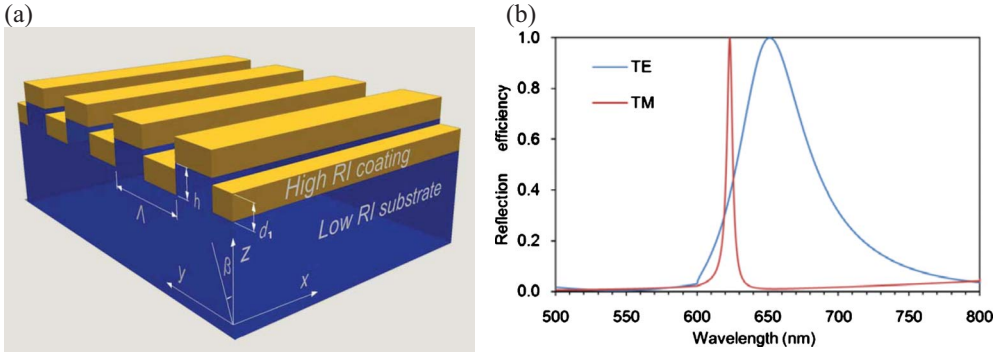

FIG. 1. (a) (Color online) Layout of the 1D planar PC displaying GMRs. (b) Calculated reflection spectra when the 1D planar PC is illuminated with TE- and TM-polarized white light at normal incidence (β=0°).

B. Glancing-angle deposition

The exploration of high-surface-area coatings for biosensor applications has been undertaken with great interest in recent years.[46–56] As the structure of a sensing film is changed from a nonstructured compact film [Fig. 3(a)] to a porous film [Fig. 3(b)], the surface area of the sensing film increases.[48] Because the response of a biosensor depends on the interaction of an analyte with an immobilized capture ligand on the sensor surface, increasing the surface area of the sensor improves the sensitivity through a higher density of the capture ligand.

GLAD[57,58] is a physical vapor deposition technique that employs glancing-angle incidence to achieve porous thin films with very high surface area. In this technique, the angle between the incoming flux and the substrate is set to be typically less than 10° [θ in Fig. 4(a)]. A random growth fluctuation in the substrate produces shadowed regions that the subsequent incident vapor flux cannot reach. When the mobility of adatoms is limited, this self-shadowing effect during deposition results in a film with a structure composed of isolated vertical nanorods tilted toward the incoming flux [Fig. 4(d)]. This technique has been used in various applications in optical and semiconductor devices.[59–73]

II. EXPERIMENTS AND RESULTS

A. Sensor structure and nanorod film deposition

The cross section of the sensor structure is illustrated in Fig. 5(a). The sensor is composed of a 1D grating in UVCP (n_{UVCP}=1.475) with a period of 550 nm and a groove depth of 170 nm, coated with 80 nm of a high-RI layer of TiO_2 (n_{TiO_2}=2.25) by sputtering. When the PC surface is immersed in water and is illuminated with TM polarized white light at normal incidence, the reflected spectrum consists of a sharp resonant peak with peak wavelength value (PWV) of 860 nm. Chemical and biomolecular materials deposited on the sensor surface result in a shift of the PWV to a longer wavelength and therefore the amount of molecules attached can be quantified.

Coating of a TiO_2 layer with nanorod structures by GLAD onto the sensor surface is performed in an electron-beam deposition system (Denton Vacuum) with a base pressure of 1.0×10^{-6} torr and a deposition rate of 10 Å/s. The incoming flux is at a glancing-angle of θ=3.0° from the sensor surface. The self-shadowing effect of the GLAD results in a nanorod structures uniformly coated on the sensor surface, as shown in the scanning electron microscope (SEM) photo of Fig. 5(b). The additional nanorod layer on the PC biosensor structure causes a positive shift of the measured PWV but it does not result in significant broadening or shortening of the resonant peak due to the small feature size of the nanorods [Fig. 5(b)].

The RI of the nanorod film, which is codeposited on a Si wafer positioned next to the sensor, is measured by a spectroscopic ellipsometer (Woollam) to be n=1.45 at a wavelength of 860 nm, while the TiO_2 films deposited by evaporation in the same system at normal incidence have a RI of n=2.25. Therefore, assuming that the nanorod film contains a mixture of TiO_2 and air, we estimate that the film is composed of a 65:35 mixture of air: TiO_2, assuming a linear relation for a combination of two materials.

In order to make a rough estimate of the surface area available due to the nanorod film, a simplified physical model was constructed based on the ellipsometer measurements of film density. If we assume that the nanorod film of thickness t consists of equally spaced rods with the same diameter d, arranged in a square lattice with equal spacing of g between adjacent rods (Fig. 6), a film with a 65:35 air: TiO_2 ratio is obtained with a rod diameter of $d\sim30$ nm and a gap of $g\sim15$ nm. We expect that a gap of $g\sim15$ nm will allow permeation by a large variety of chemical and biologi-

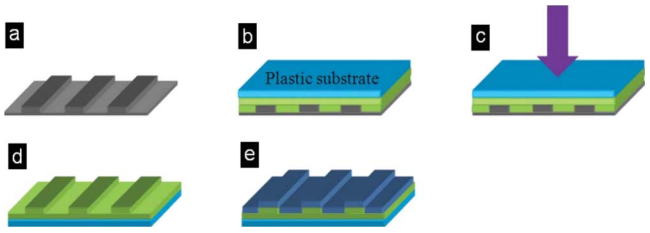

FIG. 2. (Color online) Nanoreplica molding process. (a) Si master wafer patterned. (b) UVCP sandwiched between master and substrate. (c) Polymer cured by UV illumination. (d) Substrate with grating structure peeled away from the master. (e) High-RI TiO_2 deposited by sputtering.

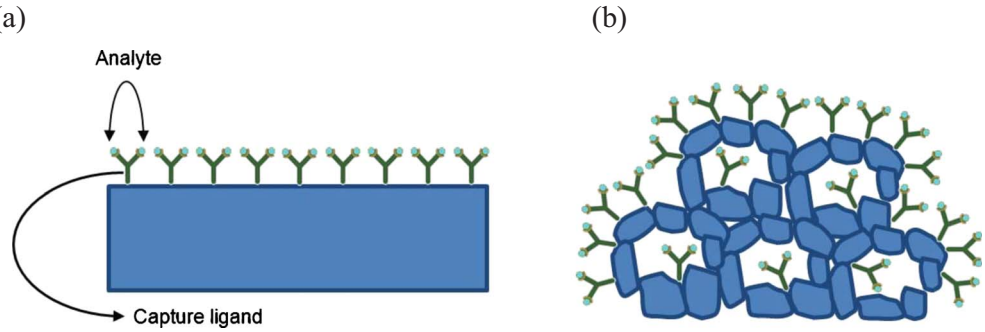

FIG. 3. (Color online) Schematics showing the effect of the surface area of a sensing film on the number of immobilized selective capture ligands for the case of (a) a nonstructured compact film and (b) a porous film.

cal materials. The extra surface area provided by each rod is the area of its sidewall, which is πdt. The ratio of total surface area of such a film with a thickness of t nm over that of a flat surface is then given by

$$\text{area factor} = \frac{\pi dt + (d+g) \times (d+g)}{(d+g) \times (d+g)} = 1 + \frac{30\pi}{45^2} \times t. \quad (1)$$

B. Poly(Phe, Lys) test

Sensitivity of the nanorod-coated sensors to surface-adsorbed material was first characterized by the detection of a single-layer film of poly(Phe, Lys) (PPL) [Sigma-Aldrich, molecular weight (MW)=35 400 Da]. PPL molecules adhere to TiO_2 surface by strong ionic bonds. In this experiment, the performance of three nanorod-coated PCs (with 60, 100, and 170 nm of nanorod) were compared with a reference PC.

Baseline PWVs were first established when all the sensors were soaked with buffer solution of 0.01*M* phosphate-buffered saline (PBS) (pH=7.4) for about 80 min. After the buffer solution was removed, a PPL solution of 0.5 mg/ml in PBS buffer was applied to the sensors' surface for about 240 min, after which weakly bound or unbound molecules were eliminated by rinsing the sensors with PBS buffer. Figure 7(a) compares the kinetic plots of each device, showing clearly that the binding kinetics of nanorod-coated sensors decrease as nanorod thickness increases. This indicates that as the nanorods get taller, it takes more time for molecules to diffuse into the porous structure and utilize the extra surface area.

Figure 7(b) shows the end point PWV shifts of all PC sensors as a function of nanorod thickness and a linear fit to the data given by

$$\text{PPL shift} = 0.0467 \times t + 1.719. \quad (2)$$

Compared with the reference sensor, which has a PPL PWV shift of 1.729 nm, a sensor coated with 57 nm of nanorod has a PWV shift of 5.044 nm, which corresponds to an enhancement factor of 2.92×. The PWV shift and enhancement factor of a 96-nm-nanorod-coated sensor are further increased to 6.202 nm and 3.59×. Finally, with the tallest nanorod used in this experiment, 167 nm, the PC sensor has a PWV shift of 9.518 nm, representing a 5.50× enhancement, compared to the reference sensor. Overall, the measured PWV shift follows a linear relation with the nanorod thickness, which suggests a surface area effect as described in Eq. (1).

C. Protein A-pig IgG assay

A bioassay that characterizes the affinity of pig immunoglobulin G (IgG) for protein A [Fig. 8(a)] is also performed to test the sensitivity of nanorod-coated sensors. Protein A is a cell wall component produced by several strains of staphylococcus aureus.[74] It consists of a single polypeptide chain and contains little or no carbohydrate. Protein A binds specifically to the Fc region of immunoglobulin molecules, especially IgG. It has four high-affinity ($K_a=10^8$/mole) binding sites that are capable of interacting with the Fc region of IgGs of several species (only two sites can bind at a time). In this experiment, pig IgG was chosen because it has a high affinity with protein A. A PC coated with 108 nm of nanorod was compared with a reference PC.

After establishing a baseline PWV with buffer solution of 0.01*M* PBS, protein A (46 700 Da, Pierce Biotechnology) prepared with 0.01*M* PBS to a concentration of 0.5 mg/ml was introduced into the sensor wells and allowed to incubate

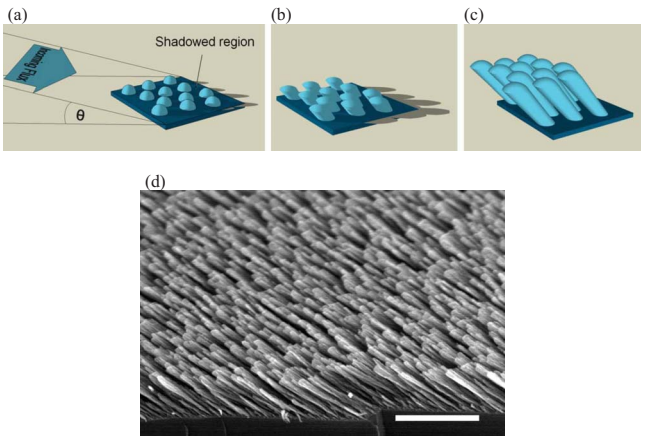

FIG. 4. [(a)–(c)] (Color online) Self-shadowing effect in GLAD. (d) A SEM image of a TiO_2 nanorod film deposited on Si substrate by GLAD.

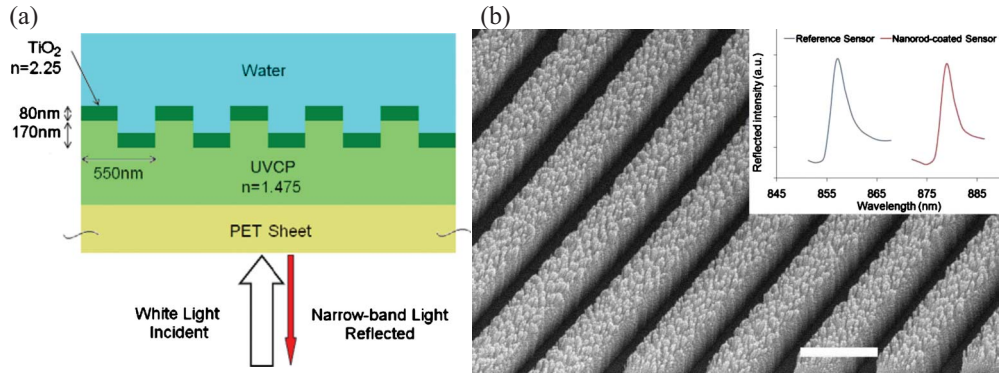

FIG. 5. (a) (Color online) Cross section of the PC label-free biosensor structure. (b) SEM photo of the nanorod-coated sensor. Scale bar=500 nm.

for 60 min. After that, weakly bound or unbound molecules were eliminated by a wash step of rinsing the sensors with PBS buffer. Pig IgG (150 000 Da, Sigma-Aldrich) serum diluted with 0.01*M* PBS to a concentration of 0.5 mg/ml was later applied onto the sensors' surface and allowed to incubate for 80 min, followed by a wash step.

Figure 8(b) shows the end point PWV shifts of the nanorod-coated and reference sensors for the protein A and pig IgG binding steps. A PWV shift of 1.82 nm was obtained from the nanorod-coated sensor due to the binding of protein A molecules, which is a 2.61× enhancement when compared to the 0.697 nm PWV shift from the reference sensor. For the pig IgG binding step, the nanorod-coated sensor had 3.221 nm of shift (1.41×) as compared to 2.287 nm on the reference sensor. This difference in enhancement indicates that the extent to which molecules could benefit from the extra surface area would depend on the size of the molecules. Assuming linear relations between the response of the sensor to these two kinds of molecules and the nanorod thickness, the following two equations can be established:

$$\text{protein A shift} = 0.0104 \times t + 0.697, \tag{3}$$

$$\text{IgG shift} = 0.0086 \times t + 2.287. \tag{4}$$

Since the size of a protein A molecule is smaller than that of a pig IgG (46 700 Da versus 150 000 Da), the slope of Eq. (3) is larger than that of Eq. (4), suggesting a molecule size effect to the enhancement of sensor sensitivity due to the nanorod coating. This reduction of enhancement for attachment of IgG to the nanorod-coated sensor indicates that large globular molecules are not able to fully take advantage of all the available surface area. Figure 9 compares the SEM photos of a nanorod-coated PC functionalized with surface chemistry layers and before (a) and after (b) application of streptavidion (SA). It is evident that after loading with globular proteins of SA, much of the space between rods is filled.

III. CONCLUSION

In this study, nanorod structure prepared by the glancing-angle deposition is used to enhance the surface area of the

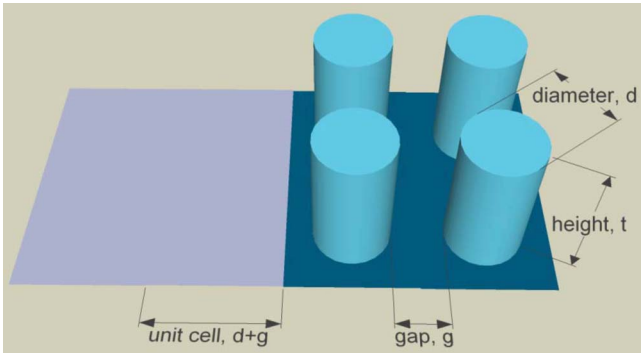

FIG. 6. (Color online) Schematic of the simplified model used to estimate the surface area of the nanorod film. Here *g* is the gap between adjacent rods, *t* is the height of the rods, and *d* is the diameter of the rods.

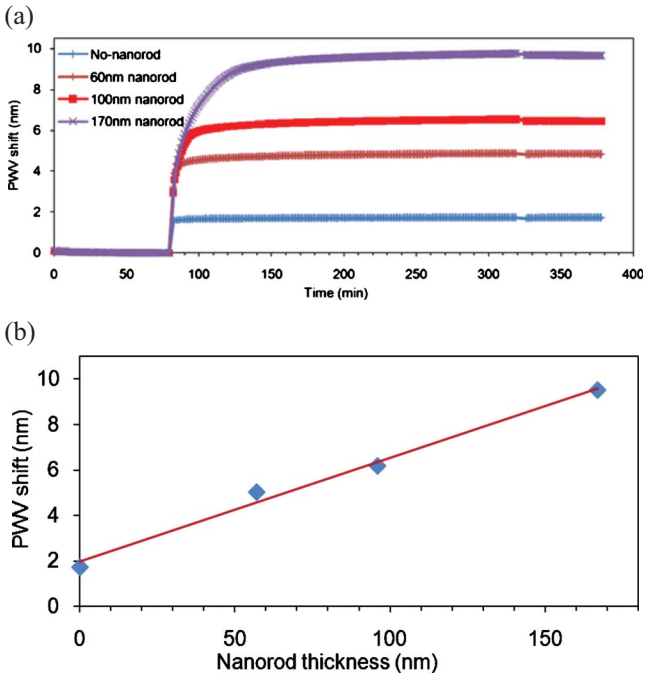

FIG. 7. (a) (Color online) Kinetic plot comparing PWV shifts for PPL deposited onto the reference PC and PCs with 60, 100, and 170 nm of nanorod coating. (b) End point PWV shift plot as a function of nanorod thickness (blue diamonds) and a linear fit (red line) to the data.

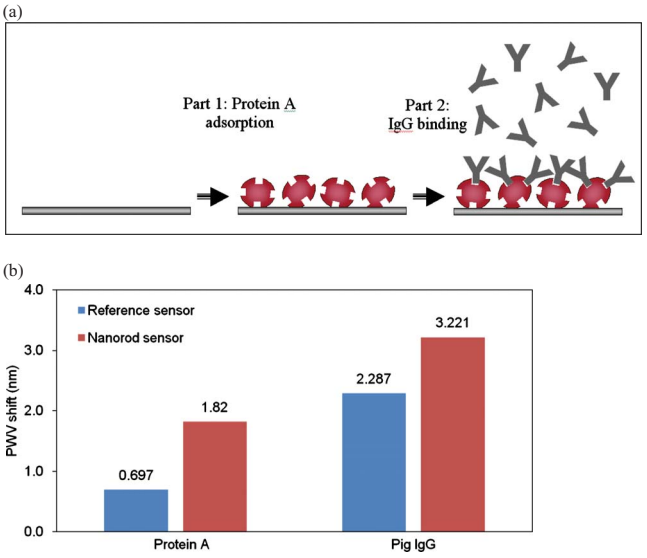

FIG. 8. (a) (Color online) Cartoon overview of experiment. In part 1, protein A is adsorbed to the sensor surface. In part 2, pig IgGs are added onto the sensor surface and their binding to protein A is measured. (b) Comparison of PWV shifts for the protein A-pig IgG interaction for a reference sensor and a sensor coated with 108 nm of nanorod.

photonic crystal biosensors. Detection of PPL and protein A-pig IgG experiments indicate a sensitivity enhancement of the sensor structure by up to 5.5 fold. The intended purpose of the nanorod coating on the PC biosensor is not primarily for decreasing the detection limits of analytes at extremely low concentrations, where detection limits are often dependent on mass transfer of scarce molecules to the sensor surface rather than the availability of a greater density of capture ligand. Rather, a greater density of immobilized ligand is advantageous in the context of pharmaceutical high throughput screening for low molecular weight chemical compounds (MW $<$ 500 Da) binding with immobilized proteins. In this application, one seeks to immobilize as large of a density of capture protein molecules as possible, where the protein, representing a critical element of a protein interaction pathway of a particular disease, is called the "target." In high throughput screening, drug discovery researchers seek to find chemical compounds that efficiently bind with the target by attaching the protein target to the biosensor surface using an appropriate surface functionalization method that results in the protein being attached to the biosensor by covalent bonds. A single chemical compound is exposed to the protein target at a concentration that is generally greater than the K_d value of the protein-molecule interaction, so a majority of the available active protein molecules will capture a small molecule. Because the immobilized protein is large (MW $>$ 50 000 Da), while the captured molecule is approximately 100 times smaller, the resulting PWV shift for the small molecule can be close to the $\sim$0.5 pm resolution of the PC biosensor. Therefore, it is advantageous to provide as large of an immobilized protein density as possible in order to obtain greater PWV shifts for small molecule binders.

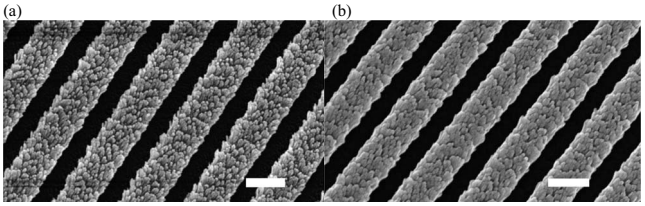

FIG. 9. SEM image for comparison of nanorod-coated PC sensors after applications of (a) surface chemistry layers and (b) SA, showing the nanorod structures are much more "loaded" after the globular proteins are deposited. Scale bars = 500 nm.

ACKNOWLEDGMENTS

This work was supported by the National Science Foundation under Grant No. 0427657. The authors gratefully acknowledge SRU Biosystems for providing financial support for this work. The authors also extend their gratitude to the support staff 317 of the Micro and Nanotechnology Laboratory at the University of Illinois at Urbana-Champaign.

[1] R. W. Wood, Philos. Mag. **4**, 392 (1902).
[2] R. W. Wood, Phys. Rev. **48**, 928 (1935).
[3] E. Popov, L. Mashev, and D. Maystre, Opt. Acta **33**, 607 (1986).
[4] H. L. Bertoni, L. H. S. Cheo, and T. Tamir, IEEE Trans. Antennas Propag. **37**, 78 (1989).
[5] S. S. Wang, R. Magnusson, J. S. Bagby, and M. G. Moharam, J. Opt. Soc. Am. A Opt. Image Sci. Vis **7**, 1470 (1990).
[6] R. Magnusson and S. S. Wang, Appl. Phys. Lett. **61**, 1022 (1992).
[7] S. S. Wang and R. Magnusson, Appl. Opt. **32**, 2606 (1993).
[8] S. Peng and G. M. Morris, J. Opt. Soc. Am. A Opt. Image Sci. Vis **13**, 993 (1996).
[9] S. Peng and G. M. Morris, Opt. Lett. **21**, 549 (1996).
[10] S. Boonruang, A. Greenwell, and M. G. Moharam, Appl. Opt. **45**, 5740 (2006).
[11] W. Suh and S. H. Fan, Appl. Phys. Lett. **84**, 4905 (2004).
[12] A. Rosenberg *et al.*, Opt. Express **13**, 6564 (2005).
[13] S. H. Fan and J. D. Joannopoulos, Phys. Rev. B **65**, 235112 (2002).
[14] V. N. Astratov, I. S. Culshaw, R. M. Stevenson, D. M. Whittaker, M. S. Skolnick, T. F. Krauss, and R. M. De la Rue, J. Lightwave Technol. **17**, 2050 (1999).
[15] F. Y. Yang, G. Yen, G. Rasigade, J. A. N. T. Soares, and B. T. Cunningham, Appl. Phys. Lett. **92**, 091115 (2008).
[16] F. Y. Yang, G. Yen, and B. T. Cunningham, Appl. Phys. Lett. **90**, 261109 (2007).
[17] A. S. P. Chang, K. J. Morton, H. Tan, P. E. Murphy, W. Wu, and S. Y. Chou, IEEE Photonics Technol. Lett. **19**, 1457 (2007).
[18] A. S. P. Chang, H. Tan, S. F. Bai, W. Wu, Z. N. Yu, and S. Y. Chou, IEEE Photonics Technol. Lett. **19**, 1099 (2007).
[19] S. Y. Chou and W. Y. Deng, Appl. Phys. Lett. **67**, 742 (1995).
[20] A. Sharon, D. Rosenblatt, A. A. Friesem, H. G. Weber, H. Engel, and R. Steingrueber, Opt. Lett. **21**, 1564 (1996).
[21] S. T. Thurman and G. M. Morris, Appl. Opt. **42**, 3225 (2003).
[22] T. Kobayashi, Y. Kanamori, and K. Hane, Appl. Phys. Lett. **87**, 151106 (2005).
[23] M. Boroditsky, T. F. Krauss, R. Coccioli, R. Vrijen, R. Bhat, and E. Yablonovitch, Appl. Phys. Lett. **75**, 1036 (1999).
[24] M. Boroditsky, R. Vrijen, T. F. Krauss, R. Coccioli, R. Bhat, and E. Yablonovitch, J. Lightwave Technol. **17**, 2096 (1999).
[25] A. A. Erchak, D. J. Ripin, S. Fan, P. Rakich, J. D. Joannopoulos, E. P. Ippen, G. S. Petrich, and L. A. Kolodziejski, Appl. Phys. Lett. **78**, 563 (2001).
[26] D. W. Carr, J. P. Sullivan, and T. A. Friedmann, Opt. Lett. **28**, 1636 (2003).
[27] B. E. N. Keeler, D. W. Carr, J. P. Sullivan, T. A. Friedmann, and J. R. Wendt, Opt. Lett. **29**, 1182 (2004).
[28] K. J. Lee, D. Wawro, P. S. Priambodo, and R. Magnusson, IEEE Sens. J. **7**, 409 (2007).

[29]B. Cunningham, B. Lin, J. Qiu, P. Li, J. Pepper, and B. Hugh, Sens. Actuators B **85**, 219 (2002).
[30]B. Cunningham, P. Li, B. Lin, and J. Pepper, Sens. Actuators B **81**, 316 (2002).
[31]I. D. Block, L. L. Chan, and B. T. Cunningham, Sens. Actuators B **120**, 187 (2006).
[32]N. Ganesh, I. D. Block, and B. T. Cunningham, Appl. Phys. Lett. **89**, 023901 (2006).
[33]W. Budach, D. Neuschafer, C. Wanke, and S. D. Chibout, Anal. Chem. **75**, 2571 (2003).
[34]D. Neuschafer, W. Budach, C. Wanke, and S. D. Chibout, Biosens. Bioelectron. **18**, 489 (2003).
[35]P. C. Mathias, N. Ganesh, L. L. Chan, and B. T. Cunningham, Appl. Opt. **46**, 2351 (2007).
[36]N. Ganesh, W. Zhang, P. C. Mathias, E. Chow, J. A. N. T. Soares, V. Malyarchuk, A. D. Smith, and B. T. Cunningham, Nat. Nanotechnol. **2**, 515 (2007).
[37]W. Zhang and B. T. Cunningham, Appl. Phys. Lett. **93**, 133115 (2008).
[38]S.-m. Kim, W. Zhang, and B. T. Cunningham, Appl. Phys. Lett. **93**, 143112 (2008).
[39]M. G. Moharam and T. K. Gaylord, J. Opt. Soc. Am. **71**, 811 (1981).
[40]N. Ganesh and B. T. Cunningham, Appl. Phys. Lett. **88**, 071110 (2006).
[41]B. T. Cunningham *et al.*, J. Biomol. Screening **9**, 481 (2004).
[42]C. J. Choi and B. T. Cunningham, Lab Chip **6**, 1373 (2006).
[43]C. J. Choi and B. T. Cunningham, Lab Chip **7**, 550 (2007).
[44]N. Ganesh, P. C. Mathias, W. Zhang, and B. T. Cunningham, J. Appl. Phys. **103**, 083104 (2008).
[45]W. Zhang, N. Ganesh, P. C. Mathias, and B. T. Cunningham, Small **4**, 2199 (2008).
[46]S. Lofas, Pure Appl. Chem. **67**, 829 (1995).
[47]S. Löfås and B. Johnsson, J. Chem. Soc., Chem. Commun. **1990**, 1526.
[48]K. D. Benkstein, C. J. Martinez, G. F. Li, D. C. Meier, C. B. Montgomery, and S. Semancik, J. Nanopart. Res. **8**, 809 (2006).
[49]V. S. Y. Lin, K. Motesharei, K. P. S. Dancil, M. J. Sailor, and M. R. Ghadiri, Science **278**, 840 (1997).
[50]I. Rendina, I. Rea, L. Rotiroti, and L. De Stefano, Physica E (Amsterdam) **38**, 188 (2007).
[51]S. Chan, Y. Li, L. J. Rothberg, B. L. Miller, and P. M. Fauchet, Mater. Sci. Eng., C **15**, 277 (2001).
[52]J. E. Lugo, M. Ocampo, A. G. Kirk, D. V. Plant, and P. M. Fauchet, J. New Mater. Electrochem. Syst. **10**, 113 (2007).
[53]S. Mathur, V. Sivakov, H. Shen, S. Barth, C. Cavelius, A. Nilsson, and P. Kuhn, Thin Solid Films **502**, 88 (2006).
[54]C. J. Martinez, B. Hockey, C. B. Montgomery, and S. Semancik, Langmuir **21**, 7937 (2005).
[55]M. R. Mohammadi, D. J. Fray, and M. C. Cordero-Cabrera, Sens. Actuators B **124**, 74 (2007).
[56]N. Levit, D. Pestov, and G. Tepper, Sens. Actuators B **82**, 241 (2002).
[57]K. Robbie, L. J. Friedrich, S. K. Dew, T. Smy, and M. J. Brett, J. Vac. Sci. Technol. A **13**, 1032 (1995).
[58]L. Abelmann and C. Lodder, Thin Solid Films **305**, 1 (1997).
[59]Y. C. Hsieh, S. Gadetsky, T. Suzuki, and M. Mansuripur, J. Appl. Phys. **81**, 3555 (1997).
[60]J. Q. Xi, J. K. Kim, E. F. Schubert, D. X. Ye, T. M. Lu, S. Y. Lin, and J. S. Juneja, Opt. Lett. **31**, 601 (2006).
[61]J. Q. Xi, M. F. Schubert, J. K. Kim, E. F. Schubert, M. F. Chen, S. Y. Lin, W. Liu, and J. A. Smart, Nat. Photonics **1**, 176 (2007).
[62]J. Q. Xi, J. K. Kim, and E. F. Schubert, Nano Lett. **5**, 1385 (2005).
[63]J. K. Kim *et al.*, Adv. Mater. (Weinheim, Ger.) **20**, 801 (2008).
[64]K. Robbie, A. J. P. Hnatiw, M. J. Brett, R. I. MacDonald, and J. N. McMullin, Electron. Lett. **33**, 1213 (1997).
[65]K. Kaminska, T. Brown, G. Beydaghyan, and K. Robbie, Appl. Opt. **42**, 4212 (2003).
[66]S. R. Kennedy, M. J. Brett, O. Toader, and S. John, Nano Lett. **2**, 59 (2002).
[67]M. O. Jensen and M. J. Brett, Opt. Express **13**, 3348 (2005).
[68]K. Robbie, D. J. Broer, and M. J. Brett, Nature (London) **399**, 764 (1999).
[69]K. D. Harris, A. C. van Popta, J. C. Sit, D. J. Broer, and M. J. Brett, Adv. Funct. Mater. **18**, 2147 (2008).
[70]Y. P. He, J. S. Wu, and Y. P. Zhao, Nano Lett. **7**, 1369 (2007).
[71]S. B. Chaney, S. Shanmukh, Y.-P. Zhao, and R. A. Dluhy, Appl. Phys. Lett. **87**, 031908 (2005).
[72]Y. P. Zhao, S. B. Chaney, S. Shanmukh, and R. A. Dluhy, J. Phys. Chem. B **110**, 3153 (2006).
[73]S. Shanmukh, L. Jones, J. Driskell, Y. P. Zhao, R. Dluhy, and R. A. Tripp, Nano Lett. **6**, 2630 (2006).
[74]http://www.piercenet.com/Products/Browse.cfm?fldID=01010306&WT.mc_id=keyname.